0026-895X/11/8003-518–528$25.00
MOLECULAR PHARMACOLOGY
Copyright © 2011 The American Society for Pharmacology and Experimental Therapeutics
Mol Pharmacol 80:518–528, 2011

Vol. 80, No. 3
71845/3707469
Printed in U.S.A.

Quantitative Prediction of Human Pregnane X Receptor and Cytochrome P450 3A4 Mediated Drug-Drug Interaction in a Novel Multiple Humanized Mouse Line[S]

Maki Hasegawa, Yury Kapelyukh, Harunobu Tahara, Jost Seibler, Anja Rode, Sylvia Krueger, Dongtao N. Lee, C. Roland Wolf, and Nico Scheer

Kyowa Hakko Kirin Co., Ltd., Shizuoka, Japan (M.H., H.T.); CXR Biosciences Limited, Dundee, United Kingdom (Y.K., D.N.L., C.R.W.); Cancer Research U.K. Molecular Pharmacology Unit, Biomedical Research Institute, Ninewells Hospital and Medical School, University of Dundee, Dundee, United Kingdom (C.R.W.); and TaconicArtemis, Köln, Germany (J.S., A.R., S.K., N.S.)

Received February 21, 2011; accepted May 31, 2011

ABSTRACT

Cytochrome P450 (P450) 3A4 is the predominant P450 enzyme expressed in human liver and intestine, and it is involved in the metabolism of approximately 50% of clinically used drugs. Because of the differences in the multiplicity of *CYP3A* genes and the poor correlation of substrate specificity of CYP3A proteins between species, the extrapolation of CYP3A-mediated metabolism of a drug from animals to man is difficult. This situation is further complicated by the fact that the predictability of the clinically common drug-drug interaction of pregnane X receptor (PXR)-mediated CYP3A4 induction by animal studies is limited as a result of marked species differences in the interaction of many drugs with this receptor. Here we describe a novel multiple humanized mouse line that combines a humanization for PXR, the closely related constitutive androstane receptor, and a replacement of the mouse *Cyp3a* cluster with a large human genomic region carrying *CYP3A4* and *CYP3A7*. We provide evidence that this model shows a human-like CYP3A4 induction response to different PXR activators, that it allows the ranking of these activators according to their potency to induce CYP3A4 expression in the human liver, and that it provides an experimental approach to quantitatively predict PXR/CYP3A4-mediated drug-drug interactions in humans.

Introduction

P450 enzymes play a major role in the oxidation of xenobiotics and endogenous compounds. In humans, 57 active P450 genes have been identified (Nelson et al., 2004), but only a limited number of those are involved in drug metabolism (Nebert and Russell, 2002). In this regard, the *CYP3A* subfamily is of particular importance. It contains four members, *CYP3A4*, *CYP3A5*, *CYP3A7*, and *CYP3A43*. Although the function of CYP3A43 is less well understood and CYP3A7 is a fetal form that is rarely expressed in adults, CYP3A5 and CYP3A4 both can contribute to the oxidative biotransformation of drugs (Nebert and Russell, 2002; Williams et al., 2002). CYP3A4 is generally regarded as the cytochrome P450 of greatest importance in drug metabolism because it is the most abundant hepatic and intestinal P450 enzyme, the substrate specificity is extremely broad, and it contributes to more than 50% of the primary metabolism of drugs currently on the market (de Wildt et al., 1999). CYP3A5 has an equal or reduced metabolic capability for CYP3A4 probe substrates (Williams et al., 2002), but it is polymorphic and is expressed in only 25% of white persons and approximately 50% of African Americans (Kuehl et al., 2001).

More than 100 putatively functional P450 genes have been described in the mouse (Nelson et al., 2004). The presence of more functional P450 genes in the mouse relative to humans is also reflected in the organization of the *Cyp3a* cluster, which in the mouse comprises eight functional genes. Seven of these, *Cyp3a57*, *-3a16*, *-3a41*, *-3a44*, *-3a11*, *-3a25,* and *-3a59*, are located in close proximity to each other within approximately 0.8 Mb of mouse chromosome 5, whereas *Cyp3a13*, although on the same chromosome, is separated

This work was supported in part by ITI Life Sciences, Scotland.
M.H. and Y.K. contributed equally to this work. C.R.W. and N.S. contributed equally to this work.
Article, publication date, and citation information can be found at http://molpharm.aspetjournals.org.
doi:10.1124/mol.111.071845.
[S] The online version of this article (available at http://molpharm.aspetjournals.org) contains supplemental material.

ABBREVIATIONS: P450, cytochrome P450; PXR, pregnane X receptor; CAR, constitutive androstane receptor; RIF, rifampicin; PCN, pregnenolone-16α-carbonitrile; hu, humanized; BAC, bacterial artificial chromosome; ES, embryonic stem; WT, wild type; PCR, polymerase chain reaction; SUL, sulfinpyrazone; PIO, pioglitazone; TRZ, triazolam; AUC, area under the plasma concentration-time curve; qRT, quantitative reverse transcriptase; MDZ, midazolam; DBF, dibenzylfluorescein; apoE, apolipoprotein E.

from the other genes by more than 7 Mb (Nelson et al., 2004). The comparison of the amino acid identity shows that a clear assignment of orthologous pairs between human and mouse CYP3A proteins is not possible (van Herwaarden et al., 2007). However, based on sequence similarity, abundance, tissue distribution, and regulation of expression, mouse *Cyp3a11* is generally considered most homologous to human *CYP3A4* (Yanagimoto et al., 1997; Anakk et al., 2004). *Cyp3a41* and *Cyp3a44* are female-specific isoforms with highest expression in the liver (Sakuma et al., 2000; Anakk et al., 2004). *Cyp3a16* is expressed in the fetal liver, but this expression is lost after birth (Itoh et al., 1994). *Cyp3a25* and *Cyp3a13* are expressed predominantly in the liver, but the levels are much lower than those of *Cyp3a11* (Yanagimoto et al., 1997; Dai et al., 2001). Expression and function of *Cyp3a57* and *Cyp3a59* are poorly characterized.

As a consequence of the differences in multiplicity, expression level, tissue distribution, sex bias, and substrate specificity of P450s in different species, it is difficult to make predictions on the oxidative metabolism of a drug in humans on the basis of results obtained in animal studies. Furthermore, marked species differences in the regulation of CYP3A expression have been observed. Two of the key proteins involved in the regulation of CYP3A4 expression are the pregnane X receptor (PXR) and the constitutive androstane receptor (CAR), which both interact with a large variety of different drugs (for review, see Stanley et al., 2006). The affinities of different ligands for these receptors vary significantly between species. For example, the macrocyclic antibiotic rifampicin (RIF) is more selective for the human receptor, whereas the synthetic C21 steroid pregnenolone-16α-carbonitrile (PCN) is a potent ligand of mouse, but not human PXR (Xie et al., 2000). These differences in nuclear receptor interaction with various compounds clearly limit the utility of animal models in the prediction of clinically relevant drug-drug interactions by PXR- or CAR-mediated induction of CYP3A4.

One way to overcome these limitations is the generation of humanized mouse models. Many such models have become available over the last few years (for review, see Cheung and Gonzalez, 2008). For example, humanized mouse models for PXR (Xie et al., 2000; Ma et al., 2007; Scheer et al., 2008, 2010), CAR (Zhang et al., 2002; Scheer et al., 2008), and CYP3A4 (Granvil et al., 2003; Yu et al., 2005; van Herwaarden et al., 2007) have been described by various groups. By combining two of these modifications, a PXR/CYP3A4 double humanized model was successfully generated (Ma et al., 2008). In this model, CYP3A4 expression was inducible by the human-specific PXR activator RIF but not by the mouse-specific PXR agonist PCN. However, the mouse *Cyp3a* genes in this model were not deleted. Consequently, both mouse and human enzymes could potentially contribute to the metabolism of a compound, resulting in a mixed profile of drug metabolism. Furthermore, CAR was not humanized in this model, limiting its use in studying nuclear receptor/CYP3A4-mediated drug-drug interactions.

Here we describe the generation of a novel CYP3A4/3A7 humanized mouse line (huCYP3A4/3A7). In contrast to previous random transgenesis approaches, we have used a sophisticated targeted-insertion strategy to replace the seven closely linked mouse *Cyp3a* genes on chromosome 5 with a human BAC carrying *CYP3A4* and *CYP3A7*. The basal hepatic CYP3A4 expression was relatively low yet highly inducible with the mouse-specific PXR activator PCN but not the human-specific activator RIF. Expression in the intestine was constitutively high and was also inducible, although compared with the liver, the magnitude of the intestinal induction response was lower. When crossed with the previously described humanized mouse models for PXR (huPXR) (Scheer et al., 2010) and CAR (huCAR) (Scheer et al., 2008), the induction response with the above inducers in the huPXR/huCAR/huCYP3A4/3A7 mouse line was reversed. We show that the huPXR/huCAR/huCYP3A4/3A7 model allows the ranking of different PXR activators according to their potency to induce CYP3A4 expression in humans and that this model might be a useful tool to quantitatively predict PXR/CYP3A4-mediated drug-drug interactions in the clinic.

Materials and Methods

Animal Husbandry. Mice were kept as described previously (Scheer et al., 2008). If animals were shipped to a different location, they were allowed to acclimatize for at least 5 days before an experimental procedure.

Vector Construction and Embryonic Stem Cell Targeting to Generate Cyp3a(−/−)/Cyp3a13(+/+) and huCYP3A4/3A7 mice. In all cases, culture and targeted mutagenesis of embryonic stem (ES) cells were carried out as described previously (Hogan et al., 1994). C57BL/6 mouse ES cells were used for all experiments. The technical details of the vector construction and ES cell work that was performed to generate Cyp3a(−/−)/Cyp3a13(+/+) and huCYP3A4/3A7 mice is described in the Supplemental Materials and Methods.

Generation and Molecular Characterization of Cyp3a(−/−)/3a13(+/+) and huCYP3A4/3A7 Mice. Chimeric Cyp3a(−/−)/3a13(+/+) and huCYP3A4/3A7 mice were generated by injection of correctly targeted ES cell clones into BALBc-blastocysts, which were transferred into foster mothers as described previously (Hogan et al., 1994). Litters from these fosters were visually inspected and chimerism was determined by hair color. Highly chimeric animals were used for further breeding in a C57BL/6 genetic background. Although Cyp3a(−/−)/3a13(+/+) chimeras were crossed to WT animals, an efficient Flp-deleter (Flpe-deleter) strain was used in the case of huCYP3A4/3A7 mice to remove the selection markers. Flpe mice express the corresponding recombinase in the germline, and they have been generated in house on a C57BL/6 genetic background. Germline transmission was obtained for both genotypes, and a successful in vivo deletion of selection markers could be confirmed for the huCYP3A4/3A7 mice. Heterozygous offspring emerging from the two mouse lines were further crossed to generate homozygous Cyp3a(−/−)/3a13(+/+) and huCYP3A4/3A7 mice, respectively. The genotype of these mouse lines was determined by combination of the PCRs listed in Supplemental Table 1.

Animals and Treatments. All animal studies were conducted in accordance with the guiding principles for the care and use of laboratory animals, and procedures were carried out either under a United Kingdom Home Office license with approval by the Ethical Review Committee, University of Dundee, or approved by the Committee for Animal Experiments in Kyowa Hakko Kirin Co., Ltd. Homozygous 8- to 12-week-old male Cyp3a(−/−)/3a13(+/+), huCYP3A4/3A7, and huPXR/huCAR/huCYP3A4/3A7 mice were used for all experiments. WT C57BL/6 animals of the same genetic background and age purchased from Harlan UK Limited (Bicester, Oxon, UK) were used for control experiments when applicable. Mice were dosed by oral administration or intraperitoneal injection with either corn oil, PCN (Sigma-Aldrich, St. Louis, MO), RIF (Sigma-Aldrich), sulfinpyrazone (SUL) (Prestwick Chemical, Illkirch, France), pioglitazone (PIO) (LKT Labs, St Paul, MN), or triazolam (TRZ) (Sigma-Aldrich) according to the specifications under *Results* and were sacrificed 24 h after the last dose.

Blood Sampling. Blood samples (approximately 15 μl) were collected from the tail vein at the time points specified under *Results*. The blood samples were centrifuged, and the plasma samples were collected. The plasma samples were stored at −20°C until analysis.

Quantification of Rifampicin, Sulfinpyrazone, Pioglitazone and Triazolam in Plasma. Plasma samples were analyzed by a liquid chromatography tandem mass spectrometry using an API Sciex 4000 (Applied Biosystems, Foster City, CA). The technical details of the analysis of the plasma samples are described in the Supplemental Materials and Methods.

Pharmacokinetic Analysis. The pharmacokinetic parameters for RIF, SUL, PIO, and TRZ were obtained by noncompartmental analysis. Log-transformed plasma concentrations were plotted against time. The slope of the elimination phase (λ_z) was estimated by linear regression. Maximum plasma concentration (C_{max}) and time to C_{max} (t_{max}) were obtained directly from the observed values. Apparent $t_{1/2}$ was obtained as $\ln 2/\lambda_z$. Area under the plasma concentration-time curve (AUC) from time 0 to the last data point ($AUC_{0\text{-}t}$) was calculated using the linear trapezoidal method. AUC after the last data point ($AUC_{\lambda z}$) was estimated by extrapolating with λ_z. The sum of $AUC_{0\text{-}t}$ and $AUC_{\lambda z}$ was regarded as $AUC_{0\text{-}\infty}$.

Quantitative Reverse Transcriptase PCR. Human *CYP3A4* and *CYP3A7* and murine *Cyp3a13* and *Cyp2c55* RNA was analyzed by quantitative reverse transcriptase-polymerase chain reaction (qRT-PCR). Liver and intestine samples were preserved in RNAlater solution (QIAGEN, Hilden, Germany) and incubated at 4°C overnight, then stored at −20°C until RNA isolation. The organ samples were homogenized, and total RNA was extracted using the QIAGEN RNeasy Plus Mini. The technical details of the analysis of the qRT-PCR are described in the Supplemental Materials and Methods.

Microsomal Preparation. Mouse liver and intestinal microsomes were prepared as described previously (Scheer et al., 2008).

Immunoblot Analysis. For Western Blot analysis, 3 μg of liver microsomal protein and duodenum microsomal protein from pooled mouse samples was separated by SDS-polyacrylamide gel electrophoresis, electrophoretically transferred to nitrocellulose membranes, and probed using a polyclonal rabbit anti-CYP3A4 (BD Gentest, Woburn, MA). The secondary antibody was anti-rabbit horseradish peroxidase conjugate (GE Healthcare, Chalfont St. Giles, Buckinghamshire, UK). Detection of immunoreactive proteins was performed by an enhanced chemiluminescence blot detection system (GE Healthcare). Human CYP3A4 baculosomes (0.1 pmol; Invitrogen, Carlsbad, CA) were used as a CYP3A4 standard.

Measurement of TRZ, Midazolam, Dibenzylfluorescein, and Testosterone Oxidation in Microsomes. The technical details of measuring the oxidation of TRZ, midazolam (MDZ), and dibenzylfluorescein (DBF) (BD Gentest) are described in the Supplemental Materials and Methods.

Statistics. Statistical significance was assessed to determine differences between mouse groups using a two-tailed, paired, Student's *t* test or a one-way analysis of variance with Dunnett test as indicated. The criterion for statistical significance was $P < 0.05$.

Results

Generation of Cyp3a(−/−)/3a13(+/+), huCYP3A4/3A7, and huPXR/huCAR/huCYP3A4/3A7 mice. Mice with a deletion of the seven closely linked mouse *Cyp3a* genes on chromosome 5 have been previously reported (Scheer et al., 2010). To summarize, these Cyp3a(−/−)/3a13(+/+) mice were created from a C57BL/6 mouse ES cell line that was double-targeted with *loxP* sites at the *Cyp3a57* and *Cyp3a59* loci. The mouse *Cyp3a* cluster with the exception of *Cyp3a13*, which is located 7 Mb away, was then deleted by subsequent Cre-mediated recombination between the *loxP* sites (Fig. 1, A–E). Using this procedure, all exons and introns from *Cyp3a57*, *Cyp3a16*, *Cyp3a41*, *Cyp3a44*, *Cyp3a11*, and *Cyp3a25* were deleted, including exons 1 to 4 and the promoter of *Cyp3a59*.

huCYP3A4/3A7 mice were generated from the *Cyp3a*-deleted ES cells described above by Cre-mediated insertion of a modified human BAC containing *CYP3A4* and *CYP3A7* via the noninteracting (heterospecific) Cre recombination sites *loxP* and *lox5171* (Lee and Saito, 1998) (Fig. 1, F–H). This approach is similar, although not identical, to the recombinase-mediated genomic replacement of the mouse α globin regulatory domain with the human synthetic region described by Wallace et al. (2007). In contrast to their approach, we flanked the mouse *Cyp3a* cluster with a pair of homospecific *loxP* sites in addition to the heterospecific *lox*-sites required for insertion of the human BAC, which in an intermediate step allowed us to delete the mouse *Cyp3a* locus as described above. Compared with the α globin humanization, this intermediate deletion step necessitated an additional round of ES cell transfection but had the additional advantage of generating the Cyp3a(−/−)/3a13(+/+) mice. Furthermore, our approach used a different selection marker system to achieve high stringency for the selection of humanized clones with a correct Cre-mediated insertion via the heterospecific *lox* sites. High stringency is important because of the low efficiency of site-specific insertion of large genomic sequences by recombinases in ES cells (Wallace et al., 2007). Although a hypoxanthine-phosphoribosyl-transferase complementation system was used previously, we employed an ATG-deficient neomycin cassette complemented by a promoter and an ATG introduced into the *Cyp3a* knockout locus. The former requires the use of a hypoxanthine-phosphoribosyl-transferase-deficient ES cell line, whereas neomycin confers resistance to G418, to which all eukaryotic cells are sensitive. Therefore, the neomycin complementation approach allowed us to use a standard C57BL/6 ES cell line and in principle is transferable to any eukaryotic cell line. The BAC that was used to generate the huCYP3A4/3A7 mice contains approximately 125 kilobases of genomic human DNA comprising the *CYP3A4* and *CYP3A7* gene and including a 37-kilobase sequence upstream of the *CYP3A4* transcriptional start site. The integrity of the inserted BAC was confirmed in targeted ES cells by Southern blot and PCR analysis, and the coding region of the *CYP3A4* gene was additionally sequenced to ensure that it is in accordance with the reference sequence listed by the Human Cytochrome P450 Allele Nomenclature Committee (http://www.cypalleles.ki.se/cyp3a4.htm).

huPXR/huCAR/huCYP3A4/3A7 mice were obtained by breeding of huCYP3A4/3A7 mice with the previously described huCAR and huPXR mice (Scheer et al., 2008, 2010). Homozygous Cyp3a(−/−)/3a13(+/+), huCYP3A4/3A7, and huPXR/huCAR/huCYP3A4/3A7 mice appeared normal, could not be distinguished from WT mice, and had normal survival rates and fertility (data not shown).

Analysis of Basal and Inducible CYP3A4 and CYP3A7 Expression in huCYP3A4/3A7 and huPXR/huCAR/huCYP3A4/3A7 Mice. Hepatic and intestinal CYP3A4 mRNA levels were quantified by qRT-PCR (TaqMan; Applied Biosystems, Foster City, CA) in adult mice treated with either vehicle, RIF (10 mg/kg i.p. daily for 3 days), or PCN (10 mg/kg i.p. daily for 2 days). The average ΔC_t values of 7.8 and 7.4 in the huCYP3A4/3A7 and huPXR/huCAR/huCYP3A4/3A7 mice suggested that the constitutive level of hepatic

CYP3A4 mRNA in both models was relatively low (Supplemental Table 2). In comparison, the average ΔC_t value for hepatic *Cyp3a11* expression in untreated WT animals was −0.7 (data not shown), suggesting a much higher level of expression than *CYP3A4* (a low ΔC_t value reflecting a high expression level). Basal *CYP3A4* ΔC_t values in the duodenum of the huCYP3A4/3A7 and huPXR/huCAR/huCYP3A4/3A7 mice were 6.6 and 5.9, respectively (Supplemental Table 2) compared with 6.2 for *Cyp3a11*. Therefore, the constitutive intestinal expression level of *CYP3A4* in the transgenic mice appears comparable with *Cyp3a11* in WT animals. As expected, no CYP3A4 mRNA was detected in the liver or intestine of Cyp3a(−/−)/3a13(+/+) or WT animals (data not shown).

A significant ~31-fold induction of CYP3A4 mRNA levels was observed in the liver of the huCYP3A4/3A7 animals treated with PCN but not in huPXR/huCAR/huCYP3A4/3A7 mice (Fig. 2A). In contrast, RIF induced hepatic CYP3A4 mRNA in the multiple humanized mice by approximately 200-fold but had no effect in the huCYP3A4/3A7 mouse line. Although the same trend in the induction profile was observed in the duodenum, this effect was less marked and was not statistically significant (Fig. 2B).

CYP3A7 mRNA could not be detected in the liver or intestine of the untreated adult huCYP3A4/3A7 or huPXR/huCAR/huCYP3A4/3A7 male mice. It is noteworthy that hepatic *CYP3A7* mRNA levels were detectable in PCN-treated huCYP3A4/3A7 mice and in RIF-treated huPXR/huCAR/huCYP3A4/3A7 animals but not vice versa (Supplemental Table 2). However, with average ΔC_t values of 13.1 in the liver of the PCN-treated huCYP3A4/3A7 mice and 10.4 in the RIF-induced huPXR/huCAR/huCYP3A4/3A7 model, the expression was almost 2000-fold lower than the induced *CYP3A4* expression in the liver of each of the corresponding mouse lines. This suggests that the induced hepatic *CYP3A7* mRNA expression in these models is very low.

We then determined CYP3A4 protein expression by Western blot analysis with a human CYP3A4-specific antibody. These data confirmed the mRNA analysis in that the hepatic CYP3A4 protein level in the vehicle-treated huCYP3A4/3A7 and huPXR/huCAR/huCYP3A4/3A7 mice was low and was strongly inducible with PCN and RIF in the huCYP3A4/3A7 and huPXR/huCAR/huCYP3A4/3A7, respectively (Fig. 2C). To compare the basal hepatic CYP3A4 protein levels in the transgenic mice with that in human liver, we also included pooled human liver microsomes from different donors as well as liver microsomes from single human donors with low (SD118) and high (SD002) CYP3A4 expression in the Western blot analysis. The results show that the basal hepatic CYP3A4 expression in the transgenic mice is higher than that in the human donor with low expression, in which expression was below the limit of detection by Western blot, but significantly lower than that in pooled human liver microsomes or in the donor with high expression. In the duodenum, the basal CYP3A4 expression level was higher in both models, and it was only marginally inducible with PCN and RIF in the huCYP3A4/3A7 huPXR/huCAR/huCYP3A4/3A7 mice, respectively (Fig. 2D). In this organ, RIF seems to decrease the CYP3A4 expression level in the huCYP3A4/3A7 model for unknown reasons. No CYP3A4 protein was de-

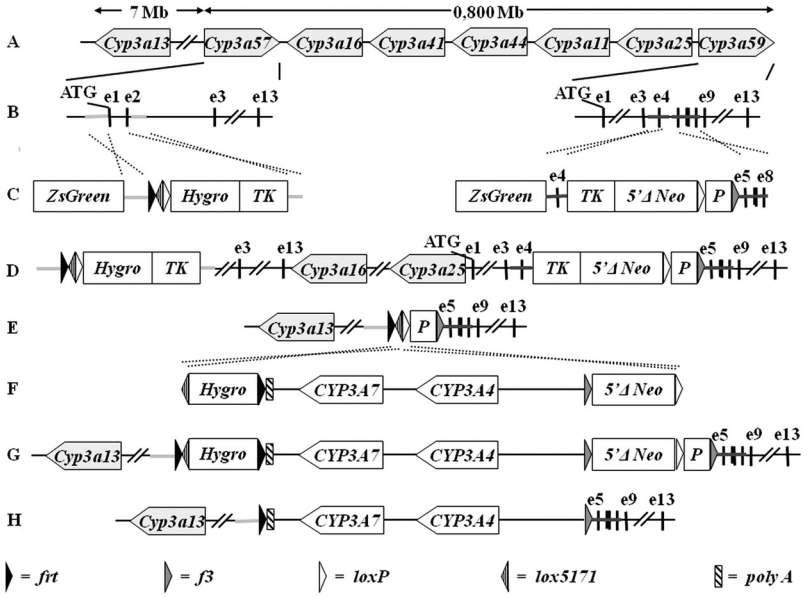

Fig. 1. Strategy to generate Cyp3a(−/−)/Cyp3a13(+/+) and huCYP3A4/3A7 mice. A, schematic representation of the chromosomal organization and orientation of functional genes within the mouse *Cyp3a* cluster. Pseudogenes are not listed. B, exon/intron structure of *Cyp3a57* and *Cyp3a59*. Exons are represented as black bars, and the ATGs mark the translational start sites of both genes. The positions of the targeting arms for homologous recombination are highlighted as light (*Cyp3a57*) and dark (*Cyp3a59*) gray lines, respectively. C, vectors used for targeting of *Cyp3a57* (left) and *Cyp3a59* (right) by homologous recombination. D, genomic organization of the *Cyp3a* cluster in double-targeted ES cells after homologous recombination on the same allele at the *Cyp3a57* and *Cyp3a59* locus. E, deletion of the mouse *Cyp3a* cluster after *Cre*-mediated recombination at the *loxP* sites. F, modified human BAC containing *CYP3A4* and *CYP3A7* used for Cre-mediated insertion into the *loxP* and *lox5171* sites of the prepared *Cyp3a* knockout locus. G, targeted mouse *Cyp3a* locus after Cre-mediated recombination of the modified human BAC into the *loxP* and *lox5171* sites of the *Cyp3a* knockout allele. H, humanized *Cyp3a* locus after Flp-mediated deletion of the *frt* and *f3*-flanked hygromycin and neomycin expression cassettes. The ES cells shown in E and H were used to generate the Cyp3a(−/−)/Cyp3a13(+/+) and huCYP3A4/3A7 mice, respectively, as described under *Materials and Methods*. For the sake of clarity, sequences are not drawn to scale. *LoxP*, *lox5171*, *frt*, and *f3* sites are represented as white, striped, black, or gray triangles, respectively. TK, thymidine kinase expression cassette; Hygro, hygromycin expression cassette; ZsGreen, ZsGreen expression cassette; P, = promoter that drives the expression of neomycin; 5′Δ Neo, ATG-deficient Neomycin.

tected in the liver or intestine of Cyp3a(−/−)/3a13(+/+) or WT animals (data not shown).

We have also investigated the induction of Cyp3a13 and Cyp2c55 mRNA expression in Cyp3a(−/−)/3a13(+/+), huCYP3A4/3A7, and huPXR/huCAR/huCYP3A4/3A7 mice, which is described in Supplemental Text 1, Supplemental Table 2, and Supplemental Fig. 1. In summary, Cyp2c55 but not Cyp3a13 mRNA expression was inducible with PCN or RIF in the corresponding treatment groups.

The CYP3A4 Protein Expressed in huCYP3A4/3A7 and huPXR/huCAR/huCYP3A4/3A7 Mice Is Catalytically Active. To further investigate the catalytic activity of the expressed CYP3A4 protein, we measured the metabolism of the CYP3A4 probe substrates TRZ, DBF, MDZ, and testosterone in microsomes from PCN- and RIF-treated animals. To assess the contribution of CYP3A4 in the metabolism of these compounds, we also included microsomes from the Cyp3a(−/−)/3a13(+/+) animals. TRZ, DBF, and MDZ oxidation determined by the formation of the metabolites α-hydroxytriazolam, fluorescein, and 4-hydroxymidazolam was significantly induced by ~4-, 3-, and 3-fold, respectively, in the liver microsomes from huCYP3A4/3A7 mice treated with PCN, but not in either the PCN-treated huPXR/huCAR/huCYP3A4/3A7 or Cyp3a(−/−)/3a13(+/+) animals (Fig. 3A). In contrast, RIF induced the oxidation of these compounds by ~24-, 18-, and 15-fold in the liver microsomes from huPXR/huCAR/huCYP3A4/3A7 mouse line only. The formation of the 1-hydroxymidazolam metabolite from MDZ and the 6β-hydroxytestosterone metabolite from testosterone was also specifically increased by ~4- and 5-fold, respectively, in the liver microsomes from PCN-treated huCYP3A4/3A7 mice and by ~11- and 29-fold in the RIF-treated huPXR/huCAR/huCYP3A4/3A7 animals (data not shown).

Similar effects were observed in the intestinal microsomes. Although the magnitude of induction after PCN treatment was comparable in the liver and duodenum, the effect of RIF

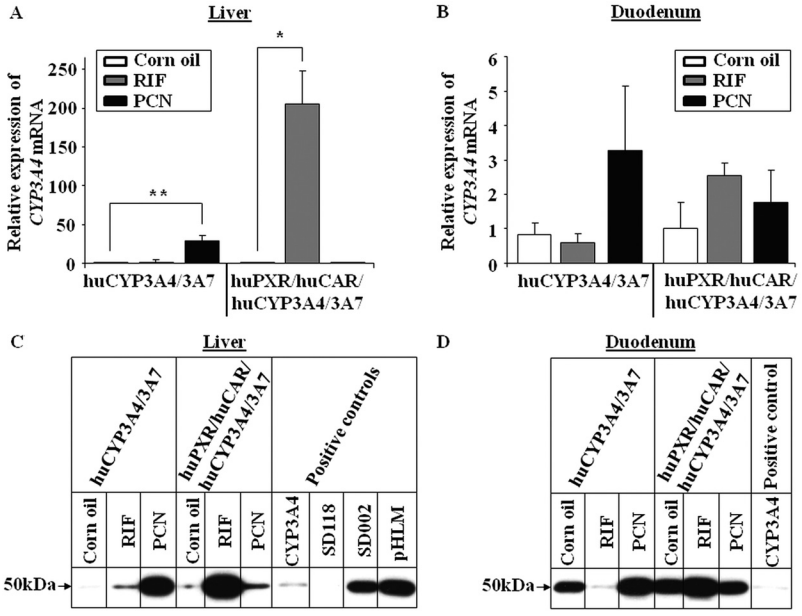

Fig. 2. CYP3A4 mRNA and protein expression levels in the liver and duodenum of huCYP3A4/3A7 and huPXR/huCAR/huCYP3A4/3A7 mice. Relative quantification of *CYP3A4* mRNA in liver (A) and duodenum (B) samples from huCYP3A4/3A7 and huPXR/huCAR/hCYP3A4/3A7 mice treated by intraperitoneal injection with either corn oil, RIF (10 mg/kg daily for 3 days), or PCN (10 mg/kg daily for 2 days). The *CYP3A4* expression level in corn oil treated huPXR/huCAR/huCYP3A4/3A7 mice was arbitrarily set as one. Data are expressed as mean ± S.D. The CYP3A4 mRNA level of samples from treated mice was compared with that from the corresponding control group with a Student's *t* test (two-sided), with * and ** statistically different from control at $p < 0.05$ and < 0.01, respectively. CYP3A4 protein expression in liver (C) and intestinal (D) microsomes from huCYP3A4/3A7 and huPXR/huCAR/huCYP3A4/3A7 mice receiving the same treatment as described above. Each lane is a sample from pooled microsomes. Three micrograms of protein were loaded for each sample. Blots were incubated in a polyclonal rabbit anti-CYP3A4 (BD Gentest). Positive controls, recombinant human CYP3A4 (Invitrogen; 0.02 pmol loaded), single donor human liver microsomes (CellzDirect; 3 μg loaded), and pooled human liver microsomes (pHLM; BD Biosciences, 3 μg loaded). In all cases, $n = 3$ for huCYP3A4/3A7 and $n = 2$ for huPXR/huCAR/huCYP3A4/3A7 mice.

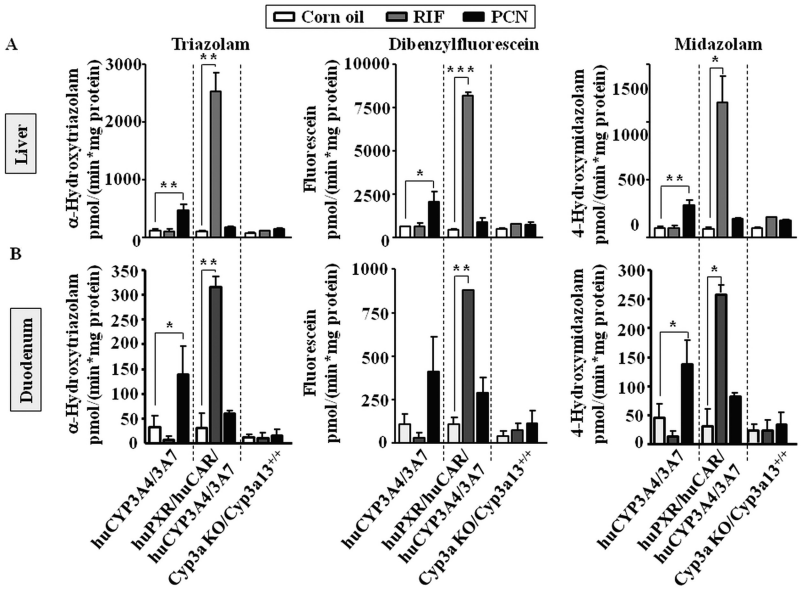

Fig. 3. Oxidation of CYP3A4 probe substrates by liver and intestinal microsomes from huCYP3A4/3A7, huPXR/huCAR/huCYP3A4/3A7, and Cyp3a(−/−)/3a13(+/+) mice. TRZ, DBF, and MDZ oxidation by liver (A) and intestinal (B) microsomes from huCYP3A4/3A7, huPXR/huCAR/hCYP3A4/3A7, and Cyp3a(−/−)/3a13(+/+) mice treated by intraperitoneal injection with either corn oil, RIF (10 mg/kg daily for 3 days), or PCN (10 mg/kg daily for 2 days) was measured by the formation of the corresponding metabolites. Data are expressed as mean ± S.D. [$n = 3$ mice for huCYP3A4/3A7 liver and intestinal microsomes and Cyp3a(−/−)/3a13(+/+)intestinal microsomes, $n = 1$ mouse for Cyp3a(−/−)/3a13(+/+) liver microsomes, and $n = 2$ mice for huPXR/huCAR/hCYP3A4/3A7 liver and intestinal microsomes]. Activities of samples from treated mice were compared with that of the corresponding control group with a Student's *t* test (two-sided), with *, **, and *** statistically different from control at $p < 0.05$, <0.01, and <0.001, respectively.

in the intestine appeared to be slightly lower than in the liver (Fig. 3B). In particular, PCN-induced α-hydroxytriazolam, fluorescein, 4-hydroxymidazolam, and 1-hydroxymidazolam formation was ~4-, 3-, 3-, and 3-fold in the duodenum of the huCYP3A4/3A7 mice and RIF-induced formation was ~10-, 8-, 9-, and 10-fold in the huPXR/huCAR/huCYP3A4/3A7 model, respectively. 6β-Hydroxytestosterone generated by duodenum microsomes was at or below the lower limit of quantification, which did not allow comparison of the activities among the experimental groups (data not shown).

In summary, these data are in general agreement with the CYP3A4 expression levels detected by qRT-PCR and Western blot analysis, and they verify that the expressed CYP3A4 protein in the humanized mouse lines is active. It is noteworthy that the intestinal induction of CYP3A4 mRNA by RIF was weak at approximately 2.5-fold, whereas the same treatment increased the catalytic activity in the microsomes from this tissue by 8- to 10-fold for TRZ, DBF, and MDZ. The reason for this difference is currently not known but cannot be due to the induction of other genes that might metabolize the CYP3A4 probe substrates, because no induction was observed in samples from the Cyp3a(−/−)/3a13(+/+) mice. The increase in catalytic activity therefore appears to be CYP3A4-dependent.

Effects of Rifampicin, Sulfinpyrazone, and Pioglitazone on Cyp3a4 Expression and Pharmacokinetics of Triazolam in huCYP3A4/3A7 and huPXR/huCAR/huCYP3A4/3A7 Mice. To assess the utility of the huPXR/huCAR/huCYP3A4/3A7 mice to rank different PXR activators according to their potency to induce CYP3A4 expression and to quantitatively predict PXR/CYP3A4-mediated drug-drug interactions in humans, the following study was carried out. huCYP3A4/3A7 (control) and huPXR/huCAR/huCYP3A4/3A7 mice were given oral daily doses of vehicle or the strong, moderate, and weak human PXR activators RIF, SUL, and PIO for 4 days (Ripp et al., 2006; Sinz et al., 2006). Serial blood samples were taken on days 1 and 4 to determine the pharmacokinetics of the compounds and to establish the doses required to obtain exposures similar to those measured in humans under standard clinical conditions. TRZ (5 mg/kg) was orally administered to all animals on day 5, followed by serial blood sampling to investigate the effect of the different PXR activators on the pharmacokinetics of this CYP3A4 probe substrate. Subsequently, the liver and intestine were prepared to measure the impact of the PXR activators on CYP3A4 expression in these organs.

The plasma concentration-time curves and pharmacokinetic parameters for RIF (tested doses 1, 3, and 10 mg/kg), SUL (0.5, 2, and 10 mg/kg), and PIO (2, 10, and 50 mg/kg) in the huPXR/huCAR/huCYP3A4/3A7 mice are shown in Fig. 4, A–C, and Table 1, respectively. For patients receiving standard clinical doses of RIF (600 mg), SUL (200 mg), and PIO (45 mg), the reported pharmacokinetic parameters were 8500 ng/ml (C_{max}) and 28,100 ng · h^{-1} · ml^{-1} ($AUC_{0-\infty}$) for RIF (Polk et al., 2001); 19,500 ng/ml (C_{max}) and 79,600 ng · h^{-1} · ml^{-1} ($AUC_{0-\infty}$) for SUL (Bradbrook et al., 1982); and 1300 to 1600 ng/ml (C_{max}) and 14,600 to 17,400 ng · h^{-1} · ml^{-1} ($AUC_{0-\infty}$) for PIO (Budde et al., 2003). On the basis of these data, we estimated that doses of 3 to 10 mg/kg RIF, 2 to 10 mg/kg SUL, and 2 mg/kg PIO resulted in exposure in mice similar to that in humans receiving a standard dose of these drugs. Furthermore, the plasma unbound fraction of RIF (0.18), SUL (0.0123), and PIO (0.015) in the huPXR/huCAR/huCYP3A4/3A7 mice was similar to that in humans (0.25 for RIF, 0.0169 for SUL, and <0.03 for PIO) (Schlicht et al., 1985; Tornio et al., 2008; Fahmi et al., 2009). The plasma concentration-time curves and pharmacokinetic parameters for the three compounds in the huCYP3A4/3A7 mice were very similar to the huPXR/huCAR/huCYP3A4/3A7 animals (data not shown).

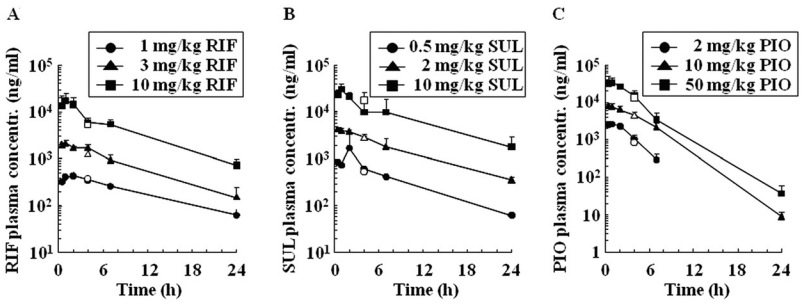

Fig. 4. Plasma concentration-time curves for different doses of rifampicin, sulfinpyrazone, and pioglitazone in huPXR/huCAR/huCYP3A4/3A7 mice. Plasma concentration-time curves in huPXR/huCAR/huCYP3A4/3A7 mice given oral doses of 1, 3, or 10 mg/kg RIF (A), 0.5, 2, or 10 mg/kg SUL (B), or 2, 10, or 50 mg/kg PIO (C). Measurements for the lowest doses are indicated as circles, those for medium dose as triangles, and those for highest dose as squares. Plasma concentration-time profiles at 4 h after administration are compared for day 1 (closed symbol) and day 4 (open symbol). For the 2 mg/kg treatment group, the PIO plasma concentration at 24 h was below the limit of detection. Each point represents the mean ± S.D. (n = 3 mice per compound and treatment).

TABLE 1

Pharmacokinetic parameters for different doses of rifampicin, sulfinpyrazone, and pioglitazone in huPXR/huCAR/huCYP3A4/3A7 mice

Data represent the mean ± S.D. (n = 3 mice per compound and treatment).

Dose	t_{max}	C_{max}	$t_{1/2}$	$AUC_{0-\infty}$
	h	ng/ml	h	$ng \cdot h^{-1} \cdot ml^{-1}$
Rifampicin				
1 mg/kg	1.3 ± 0.6	453 ± 60	8.17 ± 1.46	5920 ± 530
3 mg/kg	0.7 ± 0.3	2220 ± 230	6.18 ± 2.14	21,500 ± 1800
10 mg/kg	1.2 ± 0.8	17,600 ± 7800	6.46 ± 1.35	124,000 ± 4000
Sulfinpyrazone				
0.5 mg/kg	1.0 ± 0.9	1770 ± 1540	6.12 ± 0.39	10,400 ± 1800
2 mg/kg	0.5 ± 0.0	4250 ± 380	7.11 ± 0.97	43,200 ± 8700
10 mg/kg	1.0 ± 0.0	31,500 ± 8700	7.92 ± 1.19	230,000 ± 131,000
Pioglitazone				
2 mg/kg	0.8 ± 0.3	2680 ± 340	2.54 ± 1.67	11,400 ± 2400
10 mg/kg	0.7 ± 0.3	8460 ± 810	2.20 ± 0.13	52,900 ± 5700
50 mg/kg	1.0 ± 0.9	37,100 ± 7700	2.37 ± 0.26	154,000 ± 25,000

We then measured the effect of the different PXR activators on the *CYP3A4* mRNA levels in the liver and intestine of the two transgenic mouse lines. Compared with the vehicle-treated control mice, RIF doses of 3 and 10 mg/kg significantly increased the hepatic CYP3A4 mRNA level in the huPXR/huCAR/huCYP3A4/3A7 mouse line by 15- and 44-fold, respectively (Fig. 5A). The stronger induction of CYP3A4 mRNA expression in the liver by intraperitoneal administration of 10 mg/kg RIF (~200-fold, see above) is probably due to a higher hepatic exposure to the PXR activator after injection. Two and 10 mg/kg SUL increased the *CYP3A4* mRNA levels in the liver of this mouse line by 4.2- and 10.3-fold, respectively, but only the changes at the higher dose were statistically significant. No induction of hepatic *CYP3A4* expression was seen in the huCYP3A4/3A7 model treated with RIF or SUL, confirming that both compounds predominantly interact with the human but not the mouse PXR receptor. No significant change was observed at the relevant PIO dose of 2 mg/kg (Fig. 5A). However, the higher PIO doses of 10 and 50 mg/kg increased the hepatic CYP3A4 mRNA levels by 3.0- and 4.7-fold, with statistical significance at the 50 mg/kg dose. Accordingly, the potency of RIF, SUL, and PIO to induce *CYP3A4* expression in the liver of the huPXR/huCAR/huCYP3A4/3A7 mouse line reflects their categorization as strong, moderate, and weak activators of human PXR, respectively (Ripp et al., 2006; Sinz et al., 2006). The induction of intestinal CYP3A4 mRNA expression by the different compounds was less pronounced, and changes were generally statistically insignificant. A slight (0.6-fold) decrease of CYP3A4 mRNA was observed in the intestine of the huPXR/huCAR/huCYP3A4/3A7 treated with 50 mg/kg PIO, but the significance of this observation would need to be verified with additional studies (Fig. 5B).

The plasma concentration-time curves for TRZ in the huPXR/huCAR/huCYP3A4/3A7 mouse line after administration of RIF, SUL, and PIO are shown in Fig. 6, and the pharmacokinetic parameters are summarized in Table 2. Both RIF and SUL treatment resulted in an AUC decrease of TRZ in a dose-dependent manner. At the clinically relevant dose range of 3 to 10 mg/kg RIF, the TRZ AUC was significantly decreased by 63 to 91%. For SUL, the observed decrease in the 2 to 10 mg/kg dose range was 15 to 37%, with statistical significance at the 10 mg/kg dose. No dose-dependent effects on the TRZ AUC were observed in the huCYP3A4/3A7 model, and no changes were statistically significant (data not shown). For PIO, the decrease in the TRZ AUC in the huPXR/huCAR/huCYP3A4/3A7 model at the clinically relevant 2 mg/kg dose was 2%, whereas the 50 mg/kg dose appeared to increase the TRZ exposure. However, none of the changes observed with PIO were statistically significant.

In the RIF-treated animals, we also analyzed the changes in the pharmacokinetics of the 1-OH and α-OH TRZ metabolites. In the huPXR/huCAR/huCYP3A4/3A7 mice, but not in the huCYP3A4/3A7 animals, the AUC of both metabolites was significantly decreased (e.g., by 65 and 68%, respectively) in the 10 mg/kg treatment group (data not shown), despite the induction of CYP3A4 in this model. This is in

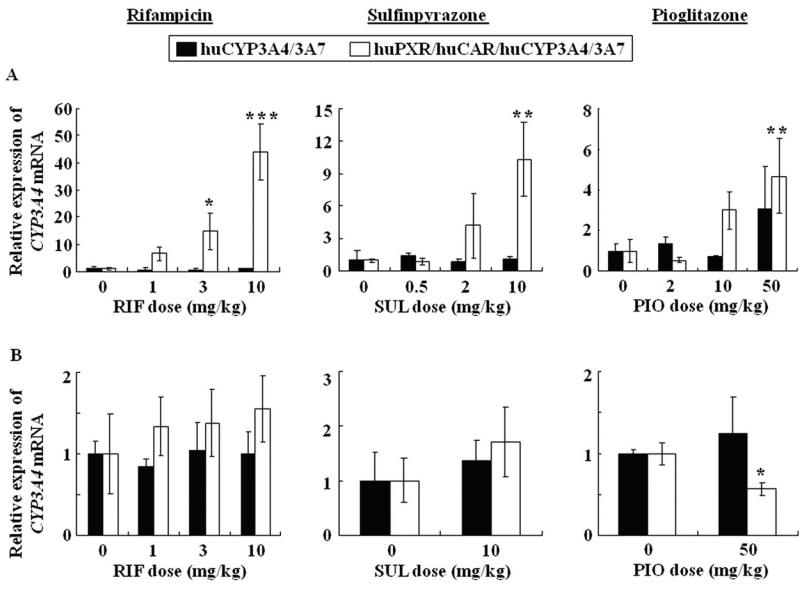

Fig. 5. Relative expression of CYP3A4 mRNA in the liver and intestine of huCYP3A4/3A7 and huPXR/huCAR/huCYP3A4/3A7 mice treated with rifampicin, sulfinpyrazone, and pioglitazone. Total RNA was isolated from the liver (A) and intestine (B) of huCYP3A4/3A7 (closed bar) and huPXR/huCAR/huCYP3A4/3A7 (open bar) mice treated with different doses of RIF, SUL, and PIO (n = 3 mice per genotype, compound and treatment). Values represent the mean expression level ± S.D. relative to the vehicle treated control group. The CYP3A4 mRNA expression levels were normalized to murine β-actin. One-way analysis of variance with Dunnett test or Student's t test was performed on the results, with *, **, and *** statistically different from control at $p < 0.05$, <0.01, and <0.001, respectively.

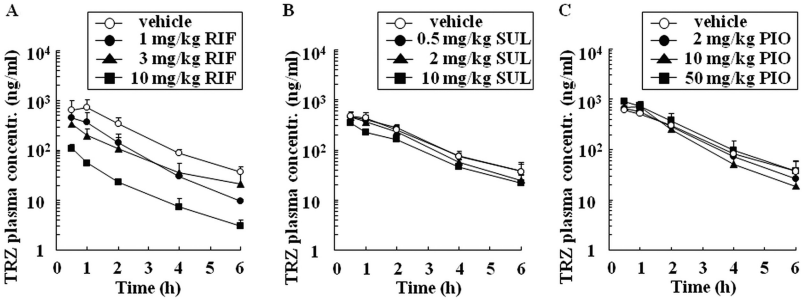

Fig. 6. Triazolam plasma concentration-time curves after different doses of rifampicin, sulfinpyrazone, and pioglitazone in huPXR/huCAR/huCYP3A4/3A7 mice. TRZ plasma concentration-time curves in huPXR/huCAR/huCYP3A4/3A7 mice given oral doses of 1, 3, or 10 mg/kg RIF (A), 0.5, 2, or 10 mg/kg SUL (B), or 2, 10, or 50 mg/kg PIO (C) and followed by a 5 mg/kg oral dose of TRZ. Measurements for the vehicle are indicated as open circles, those for the lowest doses as closed circles, those for medium dose as closed triangles, and those for the highest dose as closed squares. Each point represents the mean ± S.D. (n = 3 mice per compound and treatment).

agreement with a similar decrease in the plasma exposure of midazolam metabolites in RIF-treated cynomolgus monkeys and is probably a result of the additional induction of phase II enzymes and drug transporters by PXR (Kim et al., 2010).

Discussion

In this article, we describe the generation and characterization of a novel CYP3A4 humanized mouse line that carries a replacement of the seven chromosomally closely linked murine *Cyp3a* genes with a large human genomic region carrying *CYP3A4* and *CYP3A7*. A similar approach to replace large sequences of mouse genomic DNA with a syntenic region of human DNA was recently described for the α globin regulatory domain (Wallace et al., 2007). The use of a modified strategy allowed us to generate knockout control mice, Cyp3a(−/−)/3a13(+/+), carrying a deletion of the major part of the mouse *Cyp3a* cluster. Furthermore, because we used a different selection marker, our approach can be applied to any eukaryotic cell type and can therefore be used widely for the exchange of genomic regions between species.

The targeted insertion strategy applied in the present work distinguishes our huCYP3A4/3A7 model from other existing CYP3A4 humanized mouse lines. Compared with the random transgenic mouse line generated with the same BAC that we have used in our model (Granvil et al., 2003), the huCYP3A4/3A7 model has the advantage that it combines a knockout of the major part of the mouse *Cyp3a* cluster with the humanization of CYP3A4. This minimizes a potential contribution of mouse Cyp3a proteins to the metabolism of a CYP3A4 probe substrate in these mice. However, it should be noted that despite the absence of seven functional mouse *Cyp3a* genes in the huCYP3A4/3A7 mouse line, murine *Cyp3a13* was not deleted. The relatively low expression in the liver and intestine suggests that the relevance of Cyp3a13 in drug metabolism is limited. This assumption is supported by the fact that compared with WT animals, the catalytic activity of liver and intestinal microsomes from the Cyp3a(−/−)/3a13(+/+) mouse line for a number of different Cyp3a probe substrates was markedly reduced, indicating that the major Cyp3a activity in the knockout animals was lost (data not shown). Furthermore, in contrast to Cyp3a11, hepatic and intestinal Cyp3a13 expression was not induced in response to PXR activation. Therefore, Cyp3a13-mediated changes in the metabolism of a CYP3A4 probe substrate as a result of PXR activation should not occur.

An important implication of our cluster replacement strategy is that it significantly simplifies the combination of the *CYP3A4* humanized locus with additional transgenic modifications in a multiple humanized mouse line. Whereas the conventional approach of crossing a random insertion of a human transgene with a knockout of the corresponding mouse gene(s) requires the combination of two independently segregating genetic loci, the *Cyp3a* knockout and *CYP3A4* humanization are linked in the huCYP3A4/3A7 model. Because PXR and CAR humanized models were generated by a targeted insertion strategy as well (Scheer et al., 2008, 2010), the combination of these different modifications in the multiple humanized huPXR/huCAR/huCYP3A4/3A7 model described in the present work was straightforward.

The expression of CYP3A4 under control of its own human promoter also distinguishes the huCYP3A4/3A7 model from mouse lines in which CYP3A4 is specifically expressed in the liver or intestine by using the apoE or villin promoter, respectively (van Herwaarden et al., 2007). Although a comparison has not been made, the basal hepatic CYP3A4 expression in the apoE-CYP3A4 mouse line appears to be significantly higher than in our huCYP3A4/3A7 model. The apoE-CYP3A4 model is well suited for studies requiring a high basal expression of CYP3A4 expression in the liver. However, because CYP3A4 expression in this model is not regulated by CAR or PXR, as it usually is in humans (Moore et al., 2000), its use is precluded for the type of drug-drug interaction studies that are described here and that have an important clinical implication. In contrast to transgenic lines

TABLE 2

Pharmacokinetic parameters of triazolam for different doses of rifampicin, sulfinpyrazone, and pioglitazone in huPXR/huCAR/huCYP3A4/3A7 mice

huPXR/huCAR/huCYP3A4/3A7 mice were given different oral doses of RIF, SUL, or PIO followed by a 5 mg/kg oral dose of TRZ. Data represent the mean ± S.D. (n = 3 mice per compound and treatment). The TRZ C_{max} and AUC values from mice treated with RIF, SUL, or PIO were compared with those from the corresponding vehicle-treated control group with a one-way analysis of variance with Dunnett test.

Dose	TRZ				
	t_{max}	C_{max}	$t_{1/2}$	$AUC_{0-\infty}$	AUC Decrease
	h	*ng/ml*	*h*	$ng \cdot h^{-1} \cdot ml^{-1}$	%
Rifampicin					
0 mg/kg	1.0 ± 0.0	730 ± 341	1.26 ± 0.38	1680 ± 580	
1 mg/kg	0.5 ± 0.0	464 ± 181	1.01 ± 0.17	814 ± 356	52
3 mg/kg	0.5 ± 0.0	337 ± 131	1.49 ± 0.27	615 ± 315*	63
10 mg/kg	0.5 ± 0.0	113 ± 23*	1.23 ± 0.22	156 ± 11**	91
Sulfinpyrazone					
0 mg/kg	0.5 ± 0.0	484 ± 93	1.39 ± 0.31	1200 ± 240	
0.5 mg/kg	0.7 ± 0.3	467 ± 109	1.46 ± 0.31	1190 ± 180	1
2 mg/kg	0.5 ± 0.0	447 ± 104	1.28 ± 0.25	1020 ± 230	15
10 mg/kg	0.5 ± 0.0	351 ± 49	1.43 ± 0.26	756 ± 71*	37
Pioglitazone					
0 mg/kg	0.7 ± 0.3	624 ± 124	1.31 ± 0.31	1420 ± 240	—
2 mg/kg	0.5 ± 0.0	653 ± 163	1.15 ± 0.12	1390 ± 340	2
10 mg/kg	0.8 ± 0.3	767 ± 176	1.06 ± 0.03	1420 ± 390	0
50 mg/kg	0.5 ± 0.0	906 ± 90	1.20 ± 0.17	1890 ± 450	-33

* $P < 0.05$, significantly different from control.
** $P < 0.01$, significantly different from control.

using heterologous promoters, this interaction can be reflected by models that contain the human *CYP3A4* regulatory sequences and can therefore be important tools to study the drug-drug interactions caused by PXR-mediated induction of CYP3A4 expression in vivo. The extrapolation of the results from such studies to the human situation is further complicated by the species differences in PXR interactions that have been observed for many drugs (Stanley et al., 2006). The huPXR/huCAR/huCYP3A4/3A7 model described in the present article might offer a solution to such challenges, and it overcomes some of the limitations of previously described mouse lines in that it combines the humanizations for both PXR and CAR with CYP3A4 and is deleted for the major part of the mouse *Cyp3a* cluster.

The finding of relatively low hepatic and robust intestinal CYP3A4 expression in adult huCYP3A4/3A7 male mice is in agreement with the observations in other models using the human *CYP3A4* promoter (Granvil et al., 2003; Yu et al., 2005). The reason for the low hepatic CYP3A4 expression in transgenic mice using the human promoter is currently unknown. However, it should be noted that in humans, the basal hepatic CYP3A4 expression is highly variable, with very low levels in some individuals (Forrester et al., 1990), and we could show that the basal hepatic CYP3A4 expression in the transgenic mice lies in the range of levels that are observed in humans. Therefore, it can be speculated that the maintenance of transgenic mice in a protected environment with controlled nutrition might simply reflect the absence of exogenous PXR/CAR-inducing agents in humans, leading to low constitutive hepatic CYP3A4 levels. Other possible explanations might be the lack of interaction of certain mouse transcription factors with the human promoter or the deficiency of distant enhancer elements in the sequence that was used. CYP3A4 expression was found to be both age- and sex-dependent in the recently described random transgenic CYP3A4 humanized mouse line (Yu et al., 2005). In this model, CYP3A4 was expressed in the liver of 2- and 4-week-old transgenic female and male mice and was lost in 6-week-old male mice but continued to be constitutively expressed in adult female mice. It is noteworthy that we could not observe such a dimorphic regulation of CYP3A4 expression in the huCYP3A4/3A7 model. In our studies, hepatic CYP3A4 expression seems to be low in both male and female mice throughout development and higher in the intestine (data not shown). These potential variations between the models might be due to position effects as a consequence of different sites of integration in the mouse genome, differences in the length or integrity of the inserted human DNA sequence, genetic background, or differences in diet. However, it should be noted that we have not systematically analyzed the changes of CYP3A4 expression over time; this requires further study.

The major aim of the present work was to evaluate whether the huPXR/huCAR/huCYP3A4 model would allow the ranking of different PXR activators according to their potency to induce CYP3A4 expression and the quantitative prediction of PXR/CYP3A4-mediated drug-drug interactions in humans. A first important finding in this regard was the induction of hepatic CYP3A4 mRNA, protein, and catalytic activity by the human specific PXR activator RIF, whereas no induction response was seen with the more potent mouse PXR agonist PCN.

We then determined the doses of the strong, moderate, and weak human PXR activators RIF, SUL, and PIO, which result in comparable exposures of these compounds in the transgenic mice as seen in humans under standard clinical conditions. At the relevant doses of 3 to 10 mg/kg RIF and 2 to 10 mg/kg SUL led to a 15- to 44-fold and 4- to 10-fold induction, respectively, of hepatic CYP3A4 mRNA expression in the huPXR/huCAR/huCYP3A4/3A7 model, whereas no induction was observed in huCYP3A4/3A7 mice. At the clinically relevant dose of 2 mg/kg, PIO did not induce CYP3A4 mRNA expression in the liver of these mice. However, this expression was induced by 3.0- and 4.7-fold at the doses of 10 and 50 mg/kg, respectively, which considerably exceed the normal clinical dose. For the three compounds tested, the results in the huPXR/huCAR/huCYP3A4/3A7 mice therefore predicted the ranking of different PXR activators according to their potency to induce CYP3A4 expression in man (Ripp et al., 2006; Sinz et al., 2006).

To assess whether the huPXR/huCAR/huCYP3A4/3A7 mouse line also permits quantitative predictions of human PXR/CYP3A4-mediated drug-drug interactions, we measured the effects of the clinically relevant RIF, SUL, and PIO doses on the pharmacokinetics of the CYP3A4 probe substrate TRZ in these mice and compared these with the described changes observed in human subjects. At the relevant doses, RIF decreased the TRZ AUC by 63 to 91% and SUL by 15 to 37% in huPXR/huCAR/huCYP3A4/3A7 mice, whereas the effect of PIO was minimal and statistically insignificant. The decreases in the exposure of coadministered CYP3A4 probe substrates observed in the clinic were 73 to 96% for RIF (Hebert et al., 1992; Backman et al., 1996; Villikka et al., 1997; Kyrklund et al., 2000; Chung et al., 2006), 39% for SUL (Caforio et al., 2000), and 0 to 26% for PIO (Prueksaritanont et al., 2001 and http://www.accessdata.fda.gov/drugsatfda_docs/label/2007/021073s031lbl.pdf). Therefore, the observed effects of the different PXR activators on the pharmacokinetics of a CYP3A4 substrate in the humanized mouse line are very similar to those reported in the clinic, and the huPXR/huCAR/huCYP3A4/3A7 mouse model thus might allow quantitative predictions of such changes in humans. Compared with a study evaluating the utility of a PXR humanized mouse line for quantitative predictions of PXR-mediated drug-drug interactions (Kim et al., 2008), the model described in the present work has the advantage of combining the humanization of both the "mediator" (PXR) as well as the "target" (CYP3A4) in this process. The same group also suggested the cynomolgus monkey as an alternative system for predicting PXR-mediated induction of CYP3A4 in humans (Kim et al., 2010). The huPXR/huCAR/huCYP3A4/3A7 model might negate the use of nonhuman primates for such studies. Comparing the results from our study with clinical observations, it should be noted, however, that published human data are based on the effect of the different PXR activators on the pharmacokinetic changes of a variety of CYP3A4 probe substrates, such as cyclosporine A, simvastatin, midazolam, and TRZ. Therefore, a direct comparison of our results with human clinical data has to be made cautiously.

An interesting observation from the present study was that PIO at a dose higher than the normal clinical dose (50 mg/kg), although inducing hepatic *CYP3A4* mRNA levels by 4.7-fold, did not decrease triazolam exposure in the huPXR/huCAR/huCYP3A4/3A7 mice. A potential explanation is that

PIO is not only a CYP3A4 inducer via PXR but also a mechanism-based inhibitor of CYP3A4 (Sahi et al., 2003). Because the induction of hepatic CYP3A4 mRNA levels at this high dose is relatively weak, it is possible that the inhibitory effect of this compound predominates at these exposure levels. Therefore, another benefit of the transgenic mouse model might be its use in assessing the relative contribution of CYP3A4 induction and inhibition to the metabolism of a compound in vivo. However, further work will be required to verify this finding.

Compared with the liver, the induction of CYP3A4 mRNA in the duodenum was less pronounced, and these changes were not statistically significant. It is noteworthy that the induction of CYP3A4-specific catalytic activity in the duodenum of huCYP3A4/3A7 and huPXR/huCAR/huCYP3A4/3A7 mice treated with PCN or RIF, respectively, was more distinct and statistically significant. The reason for this difference in mRNA induction and increase in catalytic activity remains unknown. A possible explanation might be a difference in the kinetics of CYP3A4 mRNA synthesis and degradation between the liver and the intestine so that the mRNA induction in the intestine is missed as a result of the timing of sample preparation. This explanation is also in agreement with a previous study in a PXR humanized mouse model in which it was demonstrated that, compared with the liver, intestinal CYP3A expression decreased more rapidly after withdrawal of RIF (Ma et al., 2007).

The absence of *CYP3A7* transcript in the liver and intestine of untreated huCYP3A4/3A7 and huPXR/huCAR/huCYP3A4/3A7 mice is in agreement with the classification of CYP3A7 as a fetally expressed CYP3A form that is progressively lost after birth (Stevens et al., 2003). It is noteworthy that we found that CYP3A7 mRNA expression can be induced to a limited extent in the liver of the adult CYP3A4/3A7 transgenic mice by PCN or RIF, respectively. This observation is in agreement with the previous identification of a functional PXR response element in the human *CYP3A7* promoter and with the transactivation of gene expression by this element in response to PXR activators (Pascussi et al., 1999). Furthermore, our results support the potential PXR involvement in the expression of CYP3A7, which is observed occasionally in human liver (Burk et al., 2002). Nevertheless, it should be noted that the induced hepatic CYP3A7 mRNA levels in the transgenic mice are more than 3 orders of magnitude lower than the induced CYP3A4 levels in the corresponding animals, and it is therefore unlikely that CYP3A7 contributes to the metabolism of the CYP3A4 probe substrates described in this work. Because *CYP3A5* was not included in the targeting vector and 75% of white persons do not express CYP3A5, the huPXR/huCAR/huCYP3A4/3A7 model represents the majority of this group of the human population. However, it should be noted that in other ethnic groups, such as African Americans, CYP3A5 is expressed in a larger proportion of the population, which might not be accurately represented by the model.

In summary, the present article describes the generation and characterization of a novel CYP3A4 humanized mouse line that was combined with a humanization of PXR and CAR. We provide evidence that this huPXR/huCAR/huCYP3A4/3A7 model can be a useful tool to rank different PXR activators according to their potency of inducing CYP3A4 in humans and to quantitatively predict PXR/CYP3A4-mediated drug-drug interactions in the clinic. Studies to establish whether the model can be used to evaluate CYP3A4/CAR interactions are the subject of further investigations. This model adds an important additional dimension to in vitro studies by allowing the assessment of induction responses on the basis of the pharmacokinetic changes of PXR activators in vivo. Furthermore, it offers the potential of studying the effects of compounds on both CYP3A4 induction and inhibition in an integrated single model system. The huPXR/huCAR/huCYP3A4/3A7 mouse line therefore might provide a valuable adjunct in existing technologies and in the design of clinical trials in man.

Acknowledgments

We thank Anja Müller and Oliver Dahlmann (TaconicArtemis) for technical advice.

Authorship Contributions

Participated in research design: Hasegawa, Kapelyukh, Tahara, Seibler, Wolf, and Scheer.

Conducted experiments: Hasegawa, Kapelyukh, Rode, Krueger, and Lee.

Performed data analysis: Hasegawa, Kapelyukh, Tahara, Wolf, and Scheer.

Wrote or contributed to the writing of the manuscript: Hasegawa, Tahara, Wolf, and Scheer.

References

Anakk S, Kalsotra A, Kikuta Y, Huang W, Zhang J, Staudinger JL, Moore DD, and Strobel HW (2004) CAR/PXR provide directives for Cyp3a41 gene regulation differently from Cyp3a11. *Pharmacogenomics J* **4:**91–101.

Backman JT, Olkkola KT, and Neuvonen PJ (1996) Rifampin drastically reduces plasma concentrations and effects of oral midazolam. *Clin Pharmacol Ther* **59:**7–13.

Bradbrook ID, John VA, Morrison PJ, Rogers HJ, and Spector RG (1982) Pharmacokinetics of single doses of sulphinpyrazone and its major metabolites in plasma and urine. *Br J Clin Pharmacol* **13:**177–185.

Budde K, Neumayer HH, Fritsche L, Sulowicz W, Stompôr T, and Eckland D (2003) The pharmacokinetics of pioglitazone in patients with impaired renal function. *Br J Clin Pharmacol* **55:**368–374.

Burk O, Tegude H, Koch I, Hustert E, Wolbold R, Glaeser H, Klein K, Fromm MF, Nuessler AK, Neuhaus P, et al. (2002) Molecular mechanisms of polymorphic CYP3A7 expression in adult human liver and intestine. *J Biol Chem* **277:**24280–24288.

Caforio AL, Gambino A, Tona F, Feltrin G, Marchini F, Pompei E, Testolin L, Angelini A, Dalla Volta S, and Casarotto D (2000) Sulfinpyrazone reduces cyclosporine levels: a new drug interaction in heart transplant recipients. *J Heart Lung Transplant* **19:**1205–1208.

Cheung C and Gonzalez FJ (2008) Humanized mouse lines and their application for prediction of human drug metabolism and toxicological risk assessment. *J Pharmacol Exp Ther* **327:**288–299.

Chung E, Nafziger AN, Kazierad DJ, and Bertino JS, Jr. (2006) Comparison of midazolam and simvastatin as cytochrome P450 3A probes. *Clin Pharmacol Ther* **79:**350–361.

Dai D, Bai R, Hodgson E, and Rose RL (2001) Cloning, sequencing, heterologous expression, and characterization of murine cytochrome P450 3a25*(Cyp3a25), a testosterone 6beta-hydroxylase. *J Biochem Mol Toxicol* **15:**90–99.

de Wildt SN, Kearns GL, Leeder JS, and van den Anker JN (1999) Cytochrome P450 3A: ontogeny and drug disposition. *Clin Pharmacokinet* **37:**485–505.

Fahmi OA, Hurst S, Plowchalk D, Cook J, Guo F, Youdim K, Dickins M, Phipps A, Darekar A, Hyland R, et al. (2009) Comparison of different algorithms for predicting clinical drug-drug interactions, based on the use of CYP3A4 in vitro data: predictions of compounds as precipitants of interaction. *Drug Metab Dispos* **37:**1658–1666.

Forrester LM, Neal GE, Judah DJ, Glancey MJ, and Wolf CR (1990) Evidence for involvement of multiple forms of cytochrome P-450 in aflatoxin B1 metabolism in human liver. *Proc Natl Acad Sci USA* **87:**8306–8310.

Granvil CP, Yu AM, Elizondo G, Akiyama TE, Cheung C, Feigenbaum L, Krausz KW, and Gonzalez FJ (2003) Expression of the human CYP3A4 gene in the small intestine of transgenic mice: in vitro metabolism and pharmacokinetics of midazolam. *Drug Metab Dispos* **31:**548–558.

Hebert MF, Roberts JP, Prueksaritanont T, and Benet LZ (1992) Bioavailability of cyclosporine with concomitant rifampin administration is markedly less than predicted by hepatic enzyme induction. *Clin Pharmacol Ther* **52:**453–457.

Hogan BL, Beddington RS, Costantini F, and Lacy E (1994) Production of transgenic mice, in *Manipulating the Mouse Embryo: A Laboratory Manual*, pp 253–289, Cold Spring Harbor Laboratory Press, Plainview, NY.

Itoh S, Satoh M, Abe Y, Hashimoto H, Yanagimoto T, and Kamataki T (1994) A novel form of mouse cytochrome P450 3A (Cyp3a-16). Its cDNA cloning and expression in fetal liver. *Eur J Biochem* **226:**877–882.

Kim S, Dinchuk JE, Anthony MN, Orcutt T, Zoeckler ME, Sauer MB, Mosure KW,

Vuppugalla R, Grace JE Jr, Simmermacher J, et al. (2010) Evaluation of cynomolgus monkey pregnane X receptor, primary hepatocyte, and in vivo pharmacokinetic changes in predicting human CYP3A4 induction. *Drug Metab Dispos* **38:**16–24.
Kim S, Pray D, Zheng M, Morgan DG, Pizzano JG, Zoeckler ME, Chimalakonda A, and Sinz MW (2008) Quantitative relationship between rifampicin exposure and induction of Cyp3a11 in SXR humanized mice: extrapolation to human CYP3A4 induction potential. *Drug Metab Lett* **2:**169–175.
Kuehl P, Zhang J, Lin Y, Lamba J, Assem M, Schuetz J, Watkins PB, Daly A, Wrighton SA, Hall SD, et al. (2001) Sequence diversity in CYP3A promoters and characterization of the genetic basis of polymorphic CYP3A5 expression. *Nat Genet* **27:**383–391.
Kyrklund C, Backman JT, Kivistö KT, Neuvonen M, Laitila J, and Neuvonen PJ (2000) Rifampin greatly reduces plasma simvastatin and simvastatin acid concentrations. *Clin Pharmacol Ther* **68:**592–597.
Lee G and Saito I (1998) Role of nucleotide sequences of loxP spacer region in Cre-mediated recombination. *Gene* **216:**55–65.
Ma X, Cheung C, Krausz KW, Shah YM, Wang T, Idle JR, and Gonzalez FJ (2008) A double transgenic mouse model expressing human pregnane X receptor and cytochrome P450 3A4. *Drug Metab Dispos* **36:**2506–2512.
Ma X, Shah Y, Cheung C, Guo GL, Feigenbaum L, Krausz KW, Idle JR, and Gonzalez FJ (2007) The PREgnane X receptor gene-humanized mouse: a model for investigating drug-drug interactions mediated by cytochromes P450 3A. *Drug Metab Dispos* **35:**194–200.
Moore LB, Parks DJ, Jones SA, Bledsoe RK, Consler TG, Stimmel JB, Goodwin B, Liddle C, Blanchard SG, Willson TM, et al. (2000) Orphan nuclear receptors constitutive androstane receptor and pregnane X receptor share xenobiotic and steroid ligands. *J Biol Chem* **275:**15122–15127.
Nebert DW and Russell DW (2002) Clinical importance of the cytochromes P450. *Lancet* **360:**1155–1162.
Nelson DR, Zeldin DC, Hoffman SM, Maltais LJ, Wain HM, and Nebert DW (2004) Comparison of cytochrome P450 (CYP) genes from the mouse and human genomes, including nomenclature recommendations for genes, pseudogenes and alternative-splice variants. *Pharmacogenetics* **14:**1–18.
Pascussi JM, Jounaidi Y, Drocourt L, Domergue J, Balabaud C, Maurel P, and Vilarem MJ (1999) Evidence for the presence of a functional pregnane X receptor response element in the CYP3A7 promoter gene. *Biochem Biophys Res Commun* **260:**377–381.
Polk RE, Brophy DF, Israel DS, Patron R, Sadler BM, Chittick GE, Symonds WT, Lou Y, Kristoff D, and Stein DS (2001) Pharmacokinetic Interaction between amprenavir and rifabutin or rifampin in healthy males. *Antimicrob Agents Chemother* **45:**502–508.
Prueksaritanont T, Vega JM, Zhao J, Gagliano K, Kuznetsova O, Musser B, Amin RD, Liu L, Roadcap BA, Dilzer S, et al. (2001) Interactions between simvastatin and troglitazone or pioglitazone in healthy subjects. *J Clin Pharmacol* **41:**573–581.
Ripp SL, Mills JB, Fahmi OA, Trevena KA, Liras JL, Maurer TS, and de Morais SM (2006) Use of immortalized human hepatocytes to predict the magnitude of clinical drug-drug interactions caused by CYP3A4 induction. *Drug Metab Dispos* **34:**1742–1748.
Sahi J, Black CB, Hamilton GA, Zheng X, Jolley S, Rose KA, Gilbert D, LeCluyse EL, and Sinz MW (2003) Comparative effects of thiazolidinediones on in vitro P450 enzyme induction and inhibition. *Drug Metab Dispos* **31:**439–446.
Sakuma T, Takai M, Endo Y, Kuroiwa M, Ohara A, Jarukamjorn K, Honma R, and Nemoto N (2000) A novel female-specific member of the CYP3A gene subfamily in the mouse liver. *Arch Biochem Biophys* **377:**153–162.
Scheer N, Ross J, Kapelyukh Y, Rode A, and Wolf CR (2010) In vivo responses of the human and murine pregnane X receptor to dexamethasone in mice. *Drug Metab Dispos* **38:**1046–1053.
Scheer N, Ross J, Rode A, Zevnik B, Niehaves S, Faust N, and Wolf CR (2008) A novel panel of mouse models to evaluate the role of human pregnane X receptor and constitutive androstane receptor in drug response. *J Clin Invest* **118:**3228–3239.
Schlicht F, Staiger C, de Vries J, Gundert-Remy U, Hildebrandt R, Harenberg J, Wang NS, and Weber E (1985) Pharmacokinetics of sulphinpyrazone and its major metabolites after a single dose and during chronic treatment. *Eur J Clin Pharmacol* **28:**97–103.
Sinz M, Kim S, Zhu Z, Chen T, Anthony M, Dickinson K, and Rodrigues AD (2006) Evaluation of 170 xenobiotics as transactivators of human pregnane X receptor (hPXR) and correlation to known CYP3A4 drug interactions. *Curr Drug Metab* **7:**375–388.
Stanley LA, Horsburgh BC, Ross J, Scheer N, and Wolf CR (2006) PXR and CAR: nuclear receptors which play a pivotal role in drug disposition and chemical toxicity. *Drug Metab Rev* **38:**515–597.
Stevens JC, Hines RN, Gu C, Koukouritaki SB, Manro JR, Tandler PJ, and Zaya MJ (2003) Developmental expression of the major human hepatic CYP3A enzymes. *J Pharmacol Exp Ther* **307:**573–582.
Tornio A, Niemi M, Neuvonen PJ, and Backman JT (2008) Trimethoprim and the CYP2C8*3 allele have opposite effects on the pharmacokinetics of pioglitazone. *Drug Metab Dispos* **36:**73–80.
van Herwaarden AE, Wagenaar E, van der Kruijssen CM, van Waterschoot RA, Smit JW, Song JY, van der Valk MA, van Tellingen O, van der Hoorn JW, Rosing H, et al. (2007) Knockout of cytochrome P450 3A yields new mouse models for understanding xenobiotic metabolism. *J Clin Invest* **117:**3583–3592.
Villikka K, Kivistö KT, Backman JT, Olkkola KT, and Neuvonen PJ (1997) Triazolam is ineffective in patients taking rifampin. *Clin Pharmacol Ther* **61:**8–14.
Wallace HA, Marques-Kranc F, Richardson M, Luna-Crespo F, Sharpe JA, Hughes J, Wood WG, Higgs DR, and Smith AJ (2007) Manipulating the mouse genome to engineer precise functional syntenic replacements with human sequence. *Cell* **128:**197–209.
Williams JA, Ring BJ, Cantrell VE, Jones DR, Eckstein J, Ruterbories K, Hamman MA, Hall SD, and Wrighton SA (2002) Comparative metabolic capabilities of CYP3A4, CYP3A5, and CYP3A7. *Drug Metab Dispos* **30:**883–891.
Xie W, Barwick JL, Downes M, Blumberg B, Simon CM, Nelson MC, Neuschwander-Tetri BA, Brunt EM, Guzelian PS, and Evans RM (2000) Humanized xenobiotic response in mice expressing nuclear receptor SXR. *Nature* **406:**435–439.
Yanagimoto T, Itoh S, Sawada M, and Kamataki T (1997) Mouse cytochrome P450 (Cyp3a11): predominant expression in liver and capacity to activate aflatoxin B1. *Arch Biochem Biophys* **340:**215–218.
Yu AM, Fukamachi K, Krausz KW, Cheung C, and Gonzalez FJ (2005) Potential role for human cytochrome P450 3A4 in estradiol homeostasis. *Endocrinology* **146:**2911–2919.
Zhang J, Huang W, Chua SS, Wei P, and Moore DD (2002) Modulation of acetaminophen-induced hepatotoxicity by the xenobiotic receptor CAR. *Science* **298:**422–424.

Address correspondence to: Dr. Nico Scheer, TaconicArtemis, Neurather Ring 1, 51063 Koeln, Germany. E-mail: nico.scheer@taconicartemis.com